[redacted]

FIG. 1

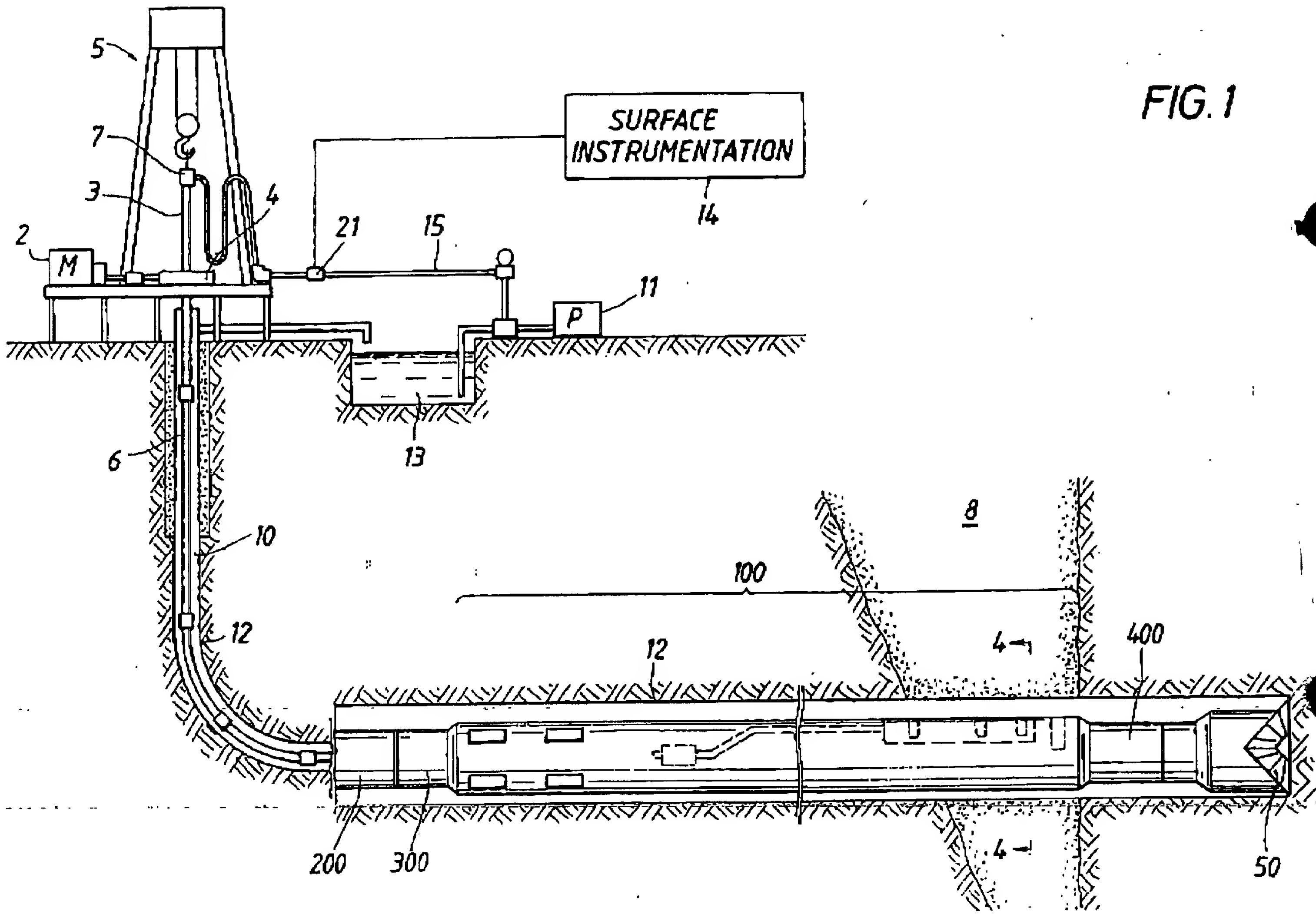

FIG. 2

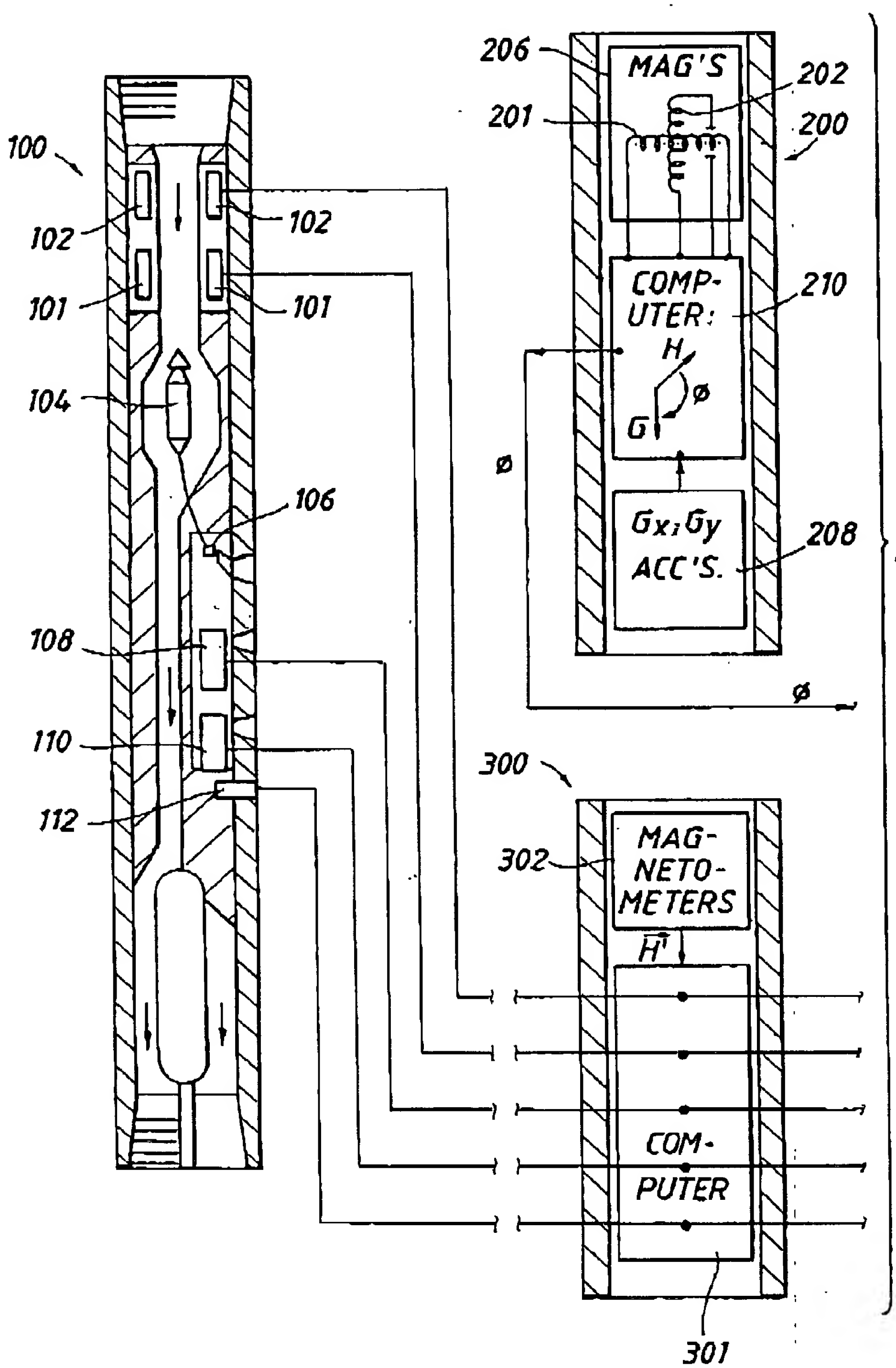
100
102
102
101
101
104
106
108
110
112
206
MAG'S
202
201
200
COMP-
UTER:
H
Ø
G
210
Ø
Gx; Gy
ACC'S.
208
Ø
300
302
MAG-
NETO-
METERS
H'
COM-
PUTER
301

FIG. 3A

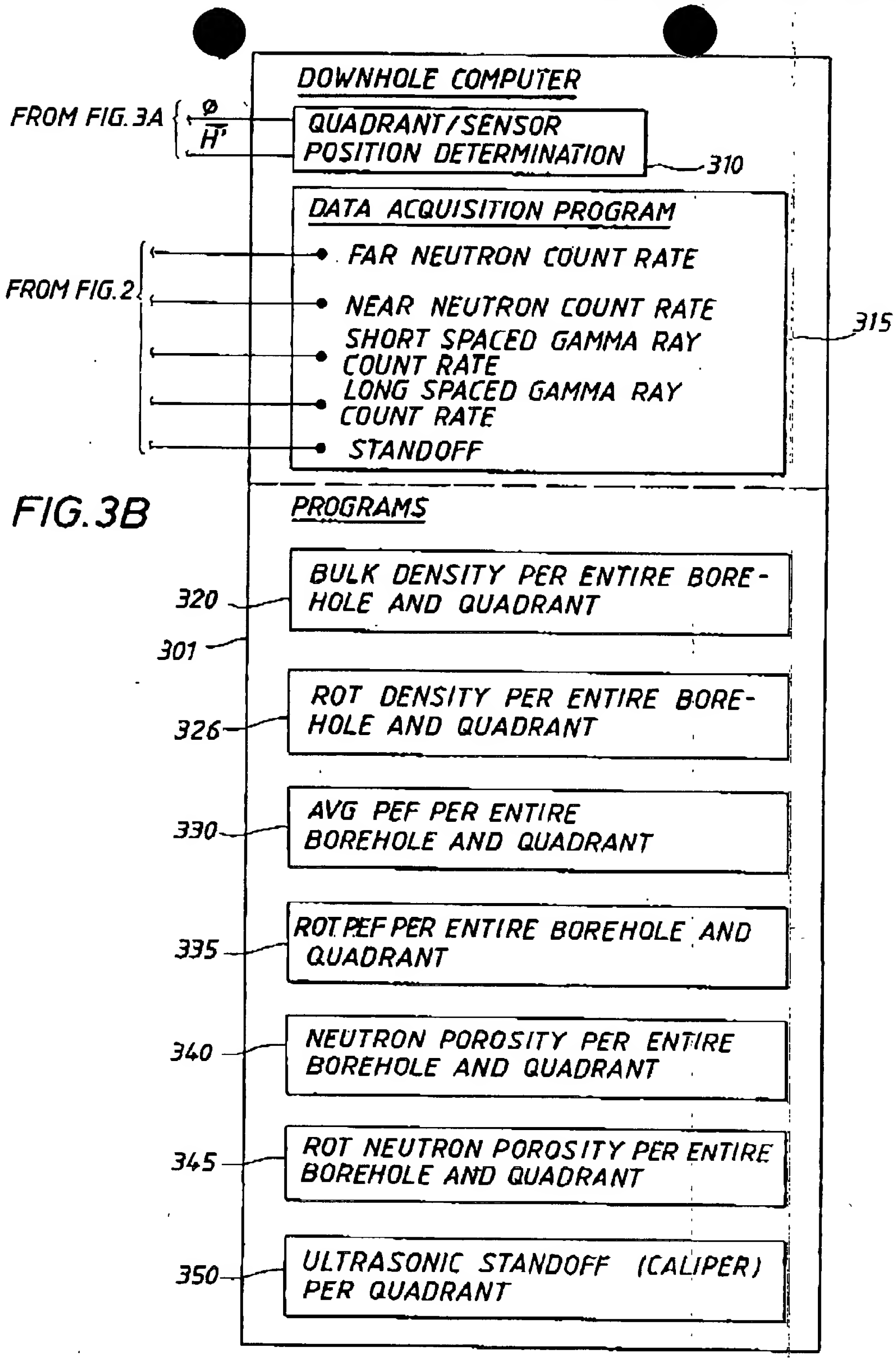
DOWNHOLE COMPUTER
FROM FIG.3A
Ø
H'
QUADRANT/SENSOR POSITION DETERMINATION
310
DATA ACQUISITION PROGRAM
FROM FIG.2
FAR NEUTRON COUNT RATE
NEAR NEUTRON COUNT RATE
SHORT SPACED GAMMA RAY COUNT RATE
LONG SPACED GAMMA RAY COUNT RATE
STANDOFF
315
PROGRAMS
320
BULK DENSITY PER ENTIRE BORE-HOLE AND QUADRANT
301
326
ROT DENSITY PER ENTIRE BORE-HOLE AND QUADRANT
330
AVG PEF PER ENTIRE BOREHOLE AND QUADRANT
335
ROT PEF PER ENTIRE BOREHOLE AND QUADRANT
340
NEUTRON POROSITY PER ENTIRE BOREHOLE AND QUADRANT
345
ROT NEUTRON POROSITY PER ENTIRE BOREHOLE AND QUADRANT
350
ULTRASONIC STANDOFF (CALIPER) PER QUADRANT

FIG.3B

FIG. 4A

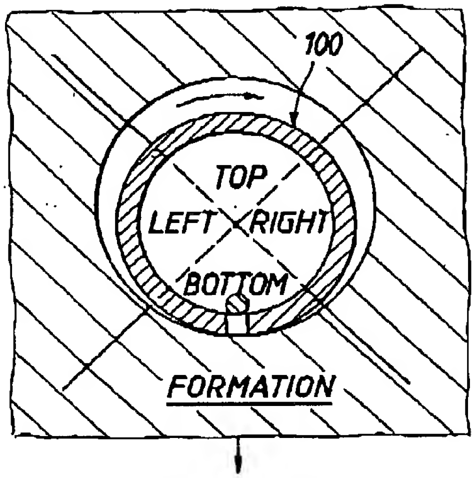

FIG. 4B

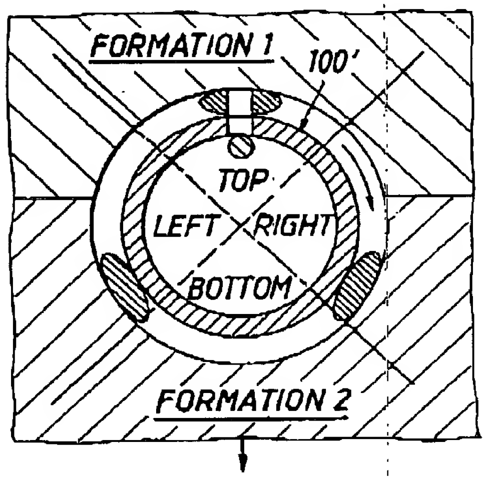

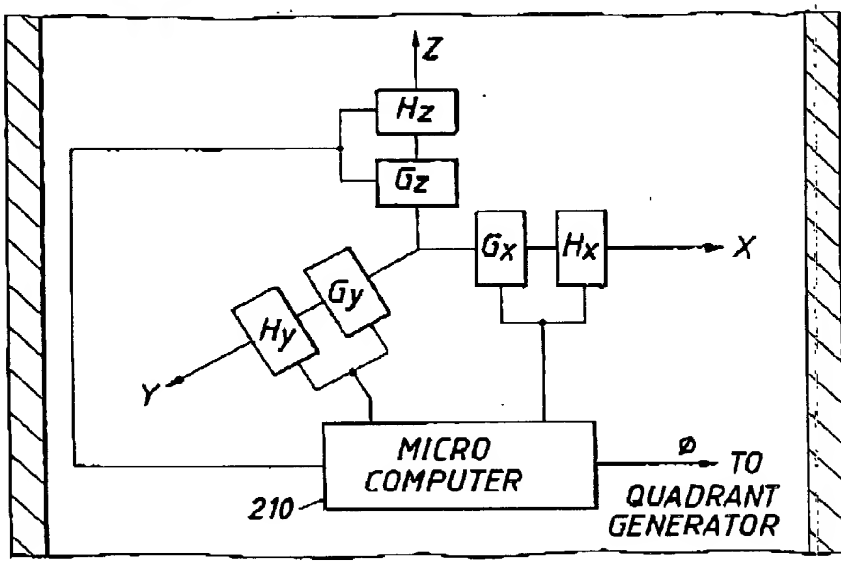

FIG. 5A

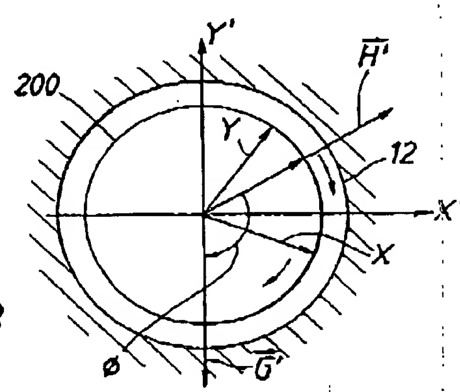

FIG. 5B

FIG. 6A

300

302

MAGNETOMETER SECTION

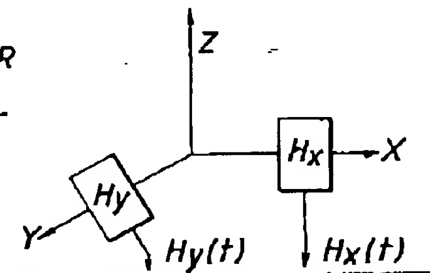

QUADRANT/SENSOR POSITION DETERMINATION COMPUTER PROGRAM

DETERMINE DOWN DIRECTION

- DETERMINE $\vec{H}'(t)$ VECTOR FROM $H_x(t)$, $H_y(t)$, $\angle\theta(t)$
- DETERMINE DOWN DIRECTION ANGLE

$$\theta = \cos^{-1} \frac{H_x(t)}{(H_x^2 + H_y^2)^{1/2}}$$

ø

$\angle\vec{H}(t) = \theta(t)$ AS MEASURED FROM TOOL X-AXIS

$\angle\vec{D}(t) = \theta(t) - \phi$ AS MEASURED FROM TOOL X-AXIS

- DETERMINE BOTTOM QUADRANT

310

$Q_{BOT}(t) = \angle\vec{D}(t) - 45°$ TO $\angle\vec{D}(t) + 45°$

$Q_{LEFT}(t) = \angle\vec{D}(t) + 45°$ TO $\angle\vec{D}(t) + 135°$

$Q_{TOP}(t) = \angle\vec{D}(t) + 135°$ TO $\angle\vec{D}(t) + 225°$

$Q_{RIGHT}(t) = \angle\vec{D}(t) + 225°$ TO $\angle\vec{D}(t) - 45°$

- DETERMINE QUADRANT OF SENSOR

$\angle\vec{S}(t)$ IS MEASURED FROM X-AXIS AND $\vec{H}(t)$ VECTOR

$\angle\vec{S}$ IS α DEGREES FROM X-AXIS

$\angle\vec{H}(t)$ IS $\theta(t)$ DEGREES FROM X-AXIS

$\angle\vec{S}(t) = \alpha$ AS MEASURED FROM X-AXIS IS

IN Q_{BOT} WHEN $\angle\vec{S}(t) = \alpha$ IS BETWEEN $\theta(t) - \phi - 45°$ AND $\theta(t) - \phi + 45°$, ETC.

FIG.6B

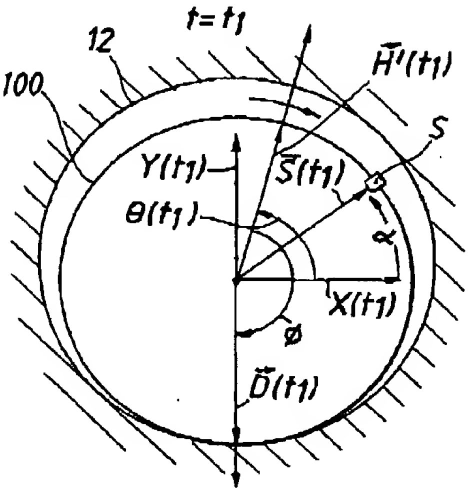

FIG.6C

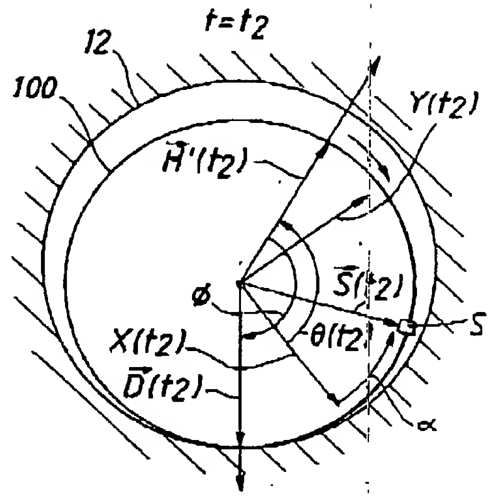

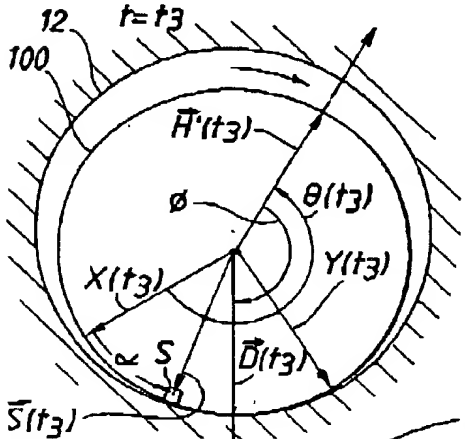

FIG.6D

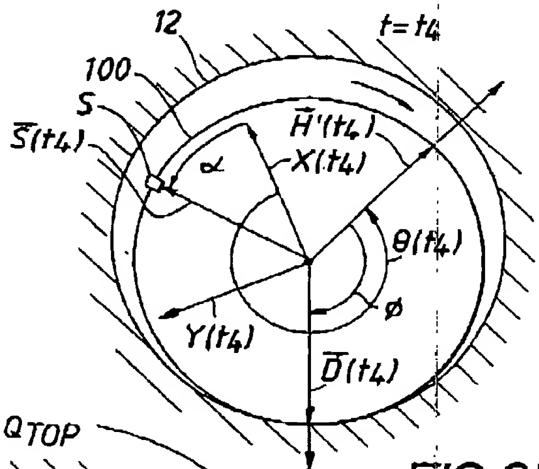

FIG.6E

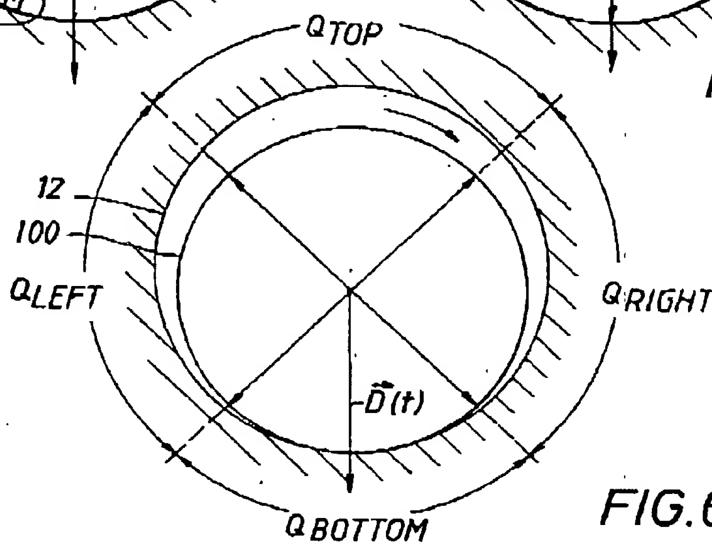

FIG.6F

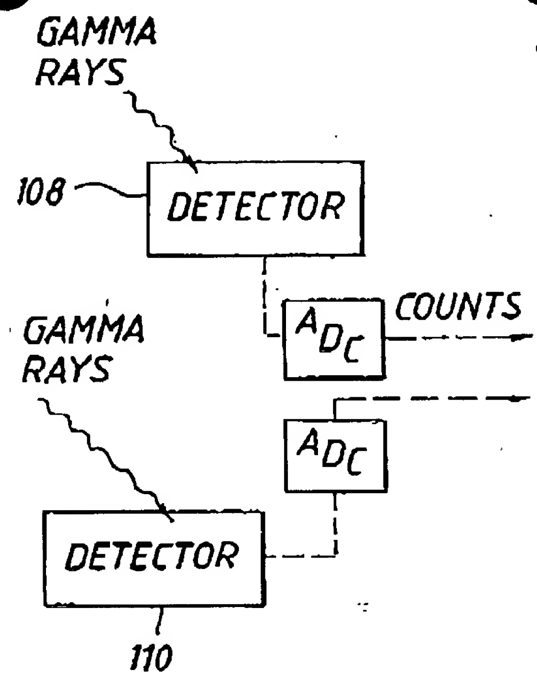
GAMMA RAYS
108
DETECTOR
ADC
COUNTS
GAMMA RAYS
ADC
DETECTOR
110

FIG. 7A

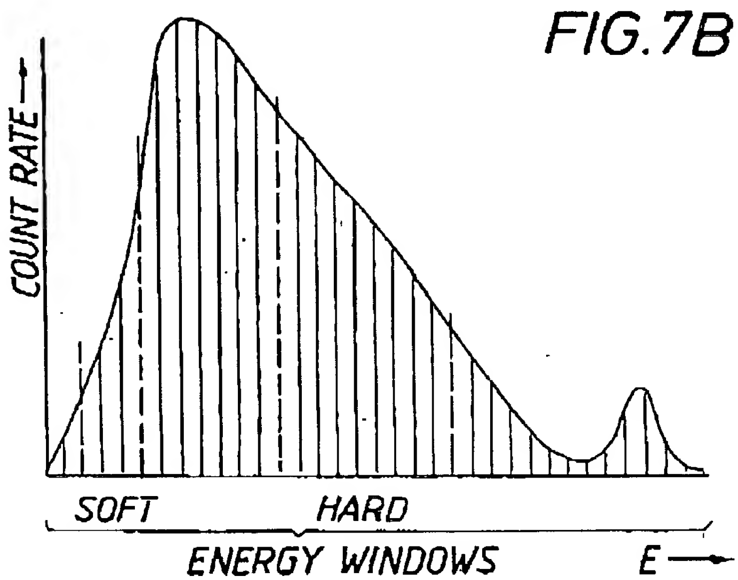
COUNT RATE
SOFT
HARD
ENERGY WINDOWS
E

FIG. 7B

FIG.8

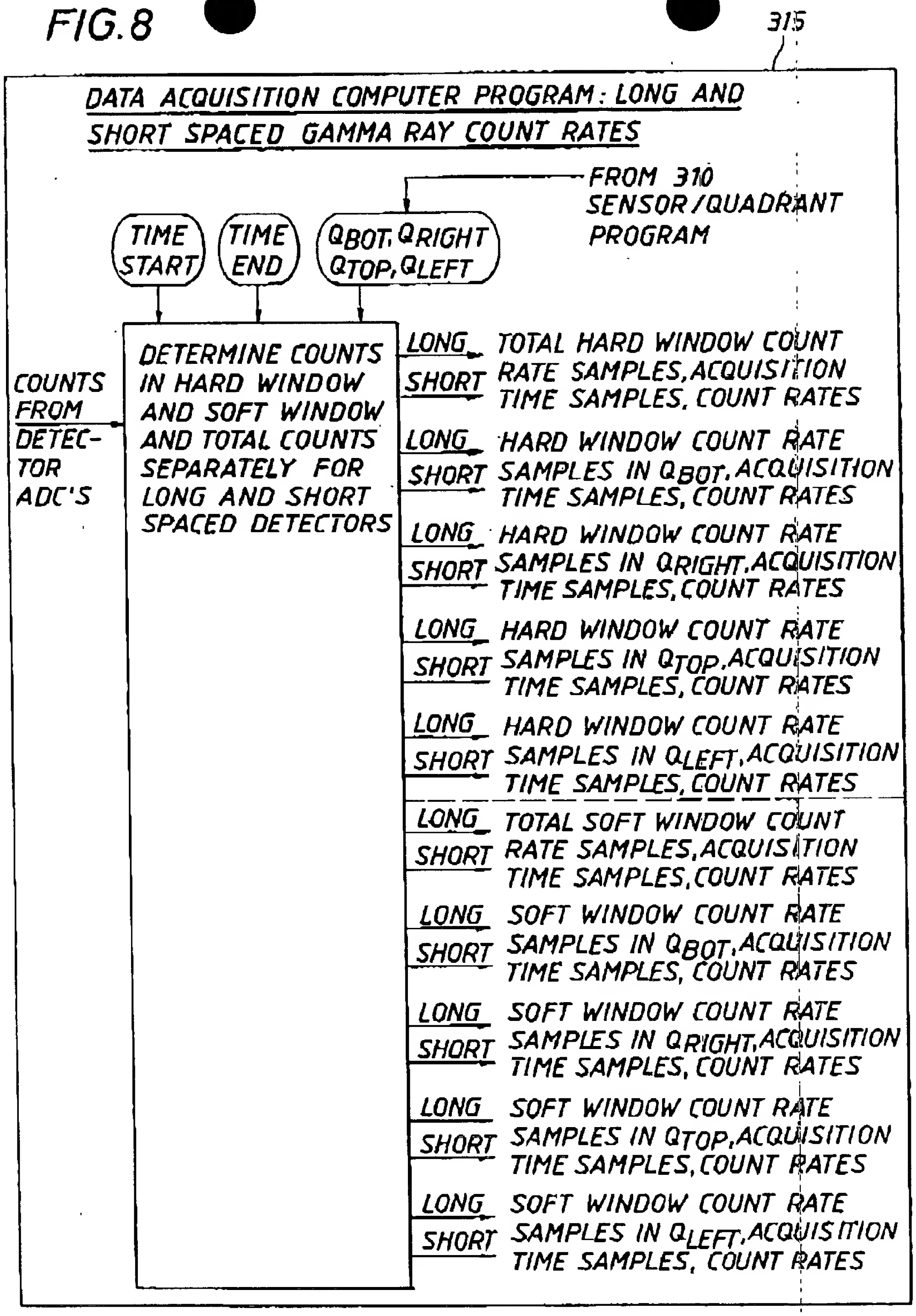
315
DATA ACQUISITION COMPUTER PROGRAM: LONG AND SHORT SPACED GAMMA RAY COUNT RATES
FROM 310 SENSOR/QUADRANT PROGRAM
TIME START
TIME END
QBOT, QRIGHT QTOP, QLEFT
COUNTS FROM DETECTOR ADC'S
DETERMINE COUNTS IN HARD WINDOW AND SOFT WINDOW AND TOTAL COUNTS SEPARATELY FOR LONG AND SHORT SPACED DETECTORS
LONG
SHORT
TOTAL HARD WINDOW COUNT RATE SAMPLES, ACQUISITION TIME SAMPLES, COUNT RATES
HARD WINDOW COUNT RATE SAMPLES IN QBOT, ACQUISITION TIME SAMPLES, COUNT RATES
HARD WINDOW COUNT RATE SAMPLES IN QRIGHT, ACQUISITION TIME SAMPLES, COUNT RATES
HARD WINDOW COUNT RATE SAMPLES IN QTOP, ACQUISITION TIME SAMPLES, COUNT RATES
HARD WINDOW COUNT RATE SAMPLES IN QLEFT, ACQUISITION TIME SAMPLES, COUNT RATES
TOTAL SOFT WINDOW COUNT RATE SAMPLES, ACQUISITION TIME SAMPLES, COUNT RATES
SOFT WINDOW COUNT RATE SAMPLES IN QBOT, ACQUISITION TIME SAMPLES, COUNT RATES
SOFT WINDOW COUNT RATE SAMPLES IN QRIGHT, ACQUISITION TIME SAMPLES, COUNT RATES
SOFT WINDOW COUNT RATE SAMPLES IN QTOP, ACQUISITION TIME SAMPLES, COUNT RATES
SOFT WINDOW COUNT RATE SAMPLES IN QLEFT, ACQUISITION TIME SAMPLES, COUNT RATES

FIG.9

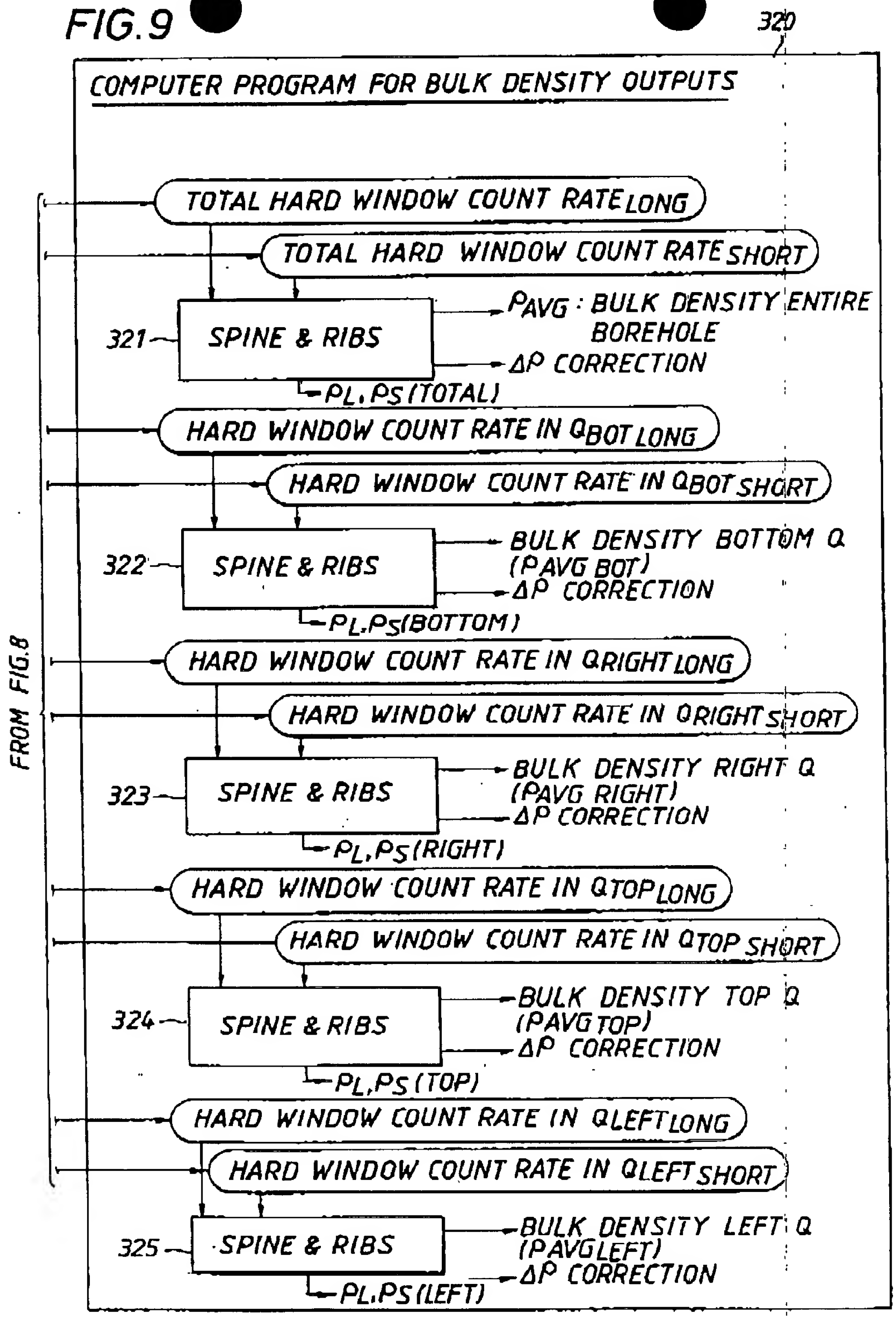
320
COMPUTER PROGRAM FOR BULK DENSITY OUTPUTS
FROM FIG.8
TOTAL HARD WINDOW COUNT RATE LONG
TOTAL HARD WINDOW COUNT RATE SHORT
321
SPINE & RIBS
ρAVG : BULK DENSITY ENTIRE BOREHOLE
Δρ CORRECTION
ρL, ρS (TOTAL)
HARD WINDOW COUNT RATE IN QBOT LONG
HARD WINDOW COUNT RATE IN QBOT SHORT
322
SPINE & RIBS
BULK DENSITY BOTTOM Q (ρAVG BOT)
Δρ CORRECTION
ρL,ρS(BOTTOM)
HARD WINDOW COUNT RATE IN QRIGHT LONG
HARD WINDOW COUNT RATE IN QRIGHT SHORT
323
SPINE & RIBS
BULK DENSITY RIGHT Q (ρAVG RIGHT)
Δρ CORRECTION
ρL,ρS (RIGHT)
HARD WINDOW COUNT RATE IN QTOP LONG
HARD WINDOW COUNT RATE IN QTOP SHORT
324
SPINE & RIBS
BULK DENSITY TOP Q (ρAVG TOP)
Δρ CORRECTION
ρL,ρS (TOP)
HARD WINDOW COUNT RATE IN QLEFT LONG
HARD WINDOW COUNT RATE IN QLEFT SHORT
325
SPINE & RIBS
BULK DENSITY LEFT Q (ρAVG LEFT)
Δρ CORRECTION
ρL,ρS (LEFT)

FIG. 10A-1

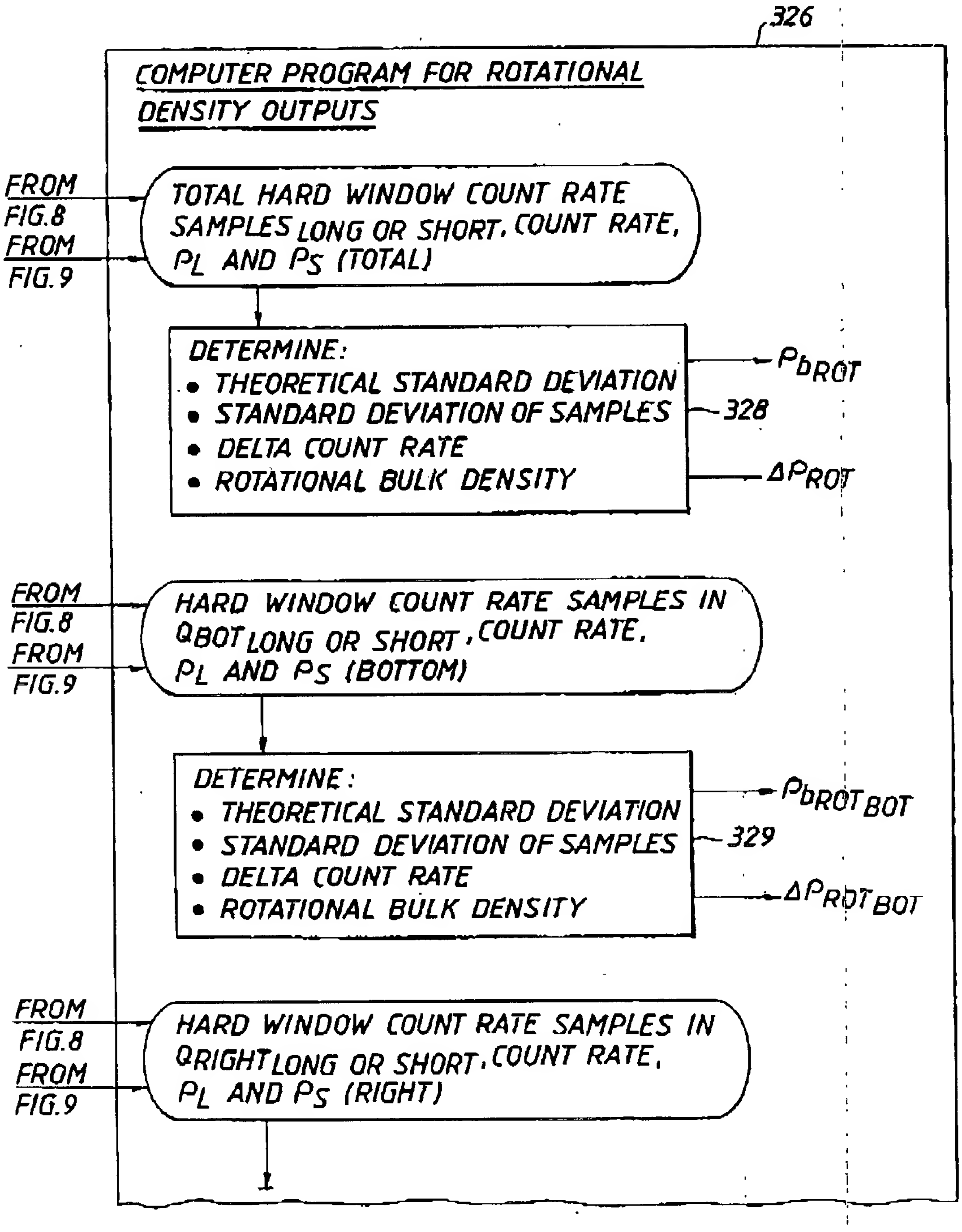

TO FIG. 10A-2

09960445 .092101

FIG.10A-2

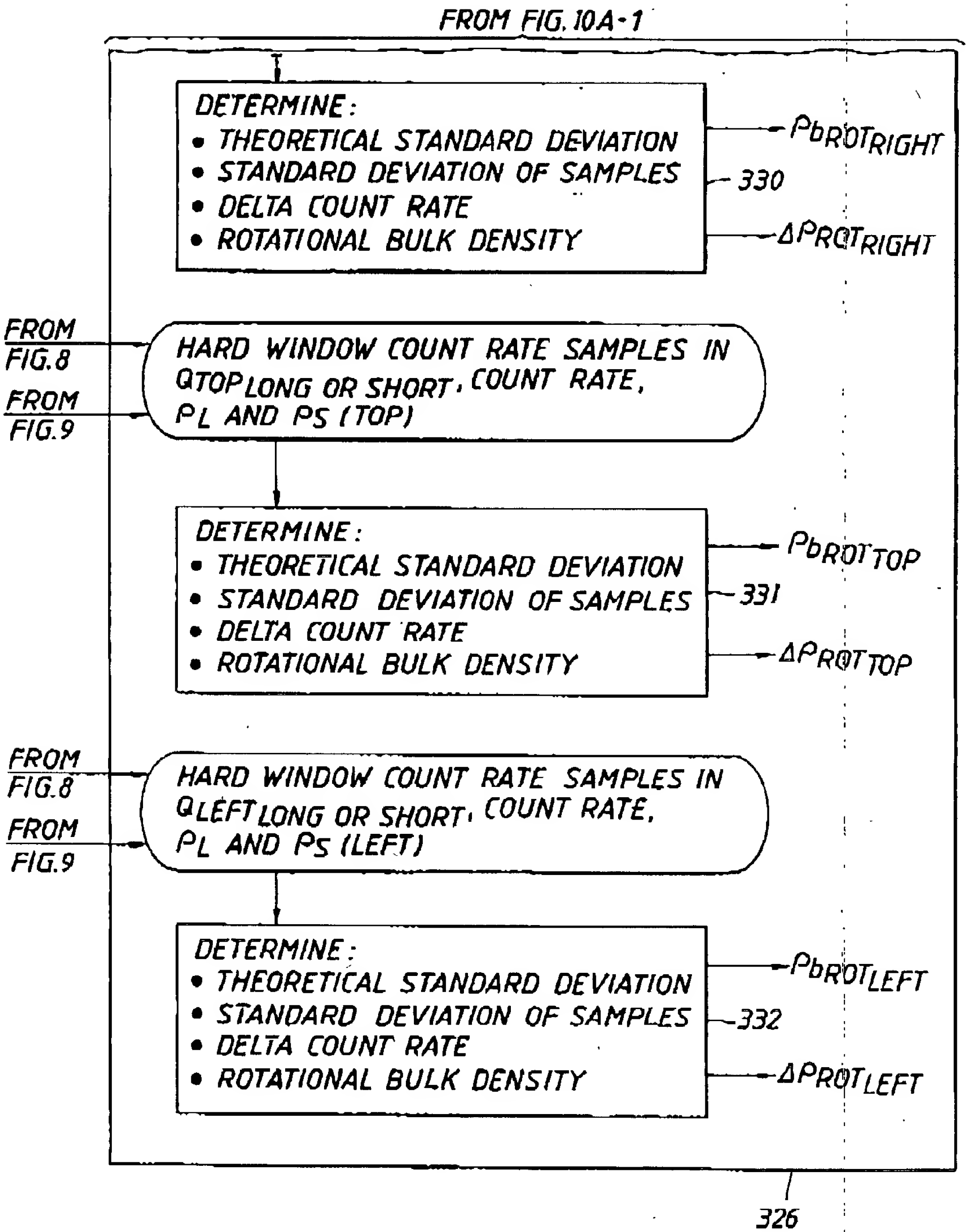

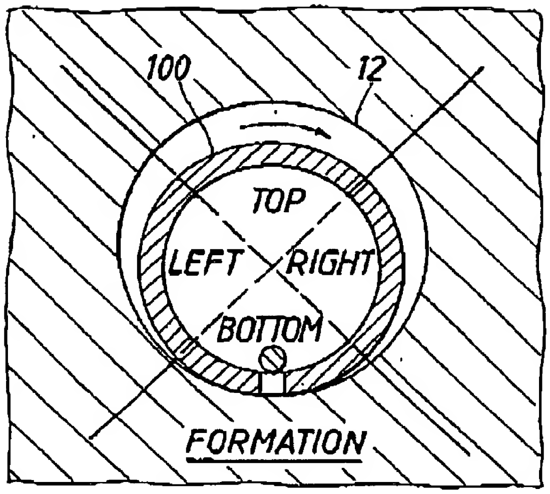

FIG.10B

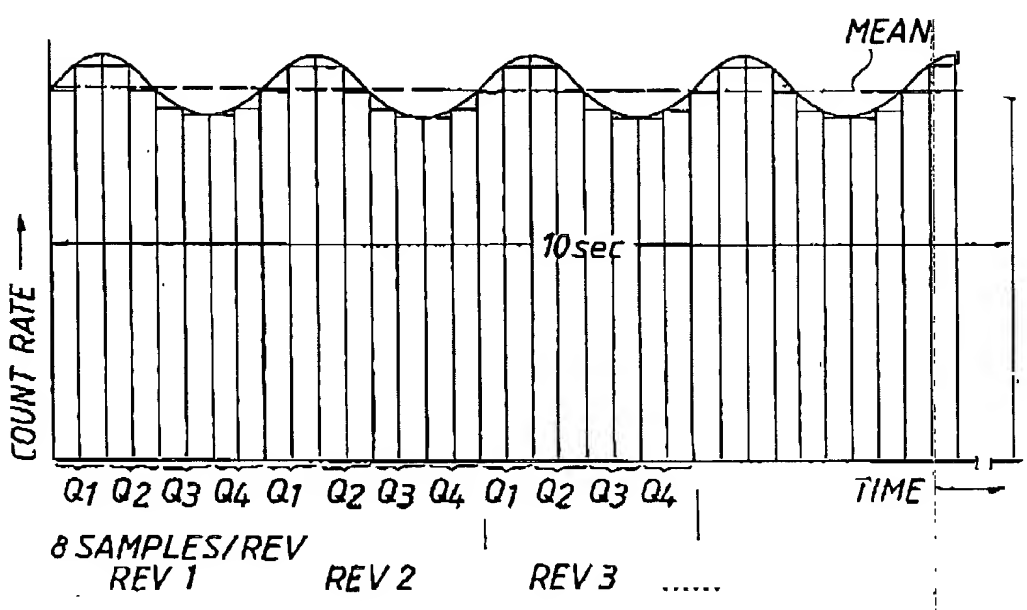

FIG.10C

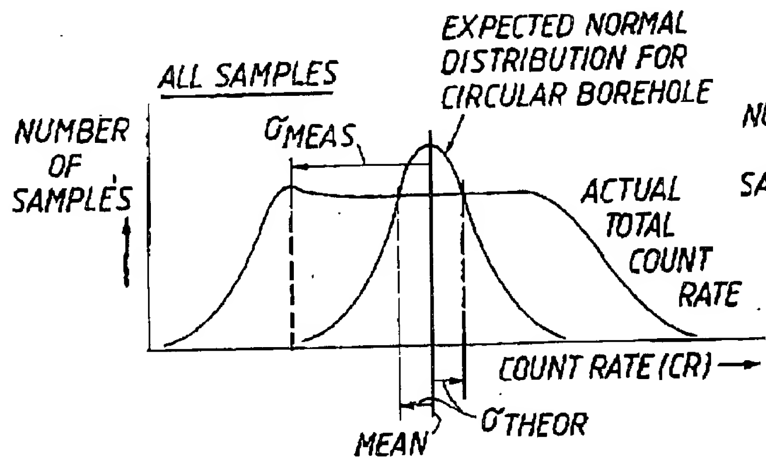

$\Delta CR = A\sqrt{\sigma^2_{MEAS} - \sigma^2_{THEOR}}$

$\Delta\rho_{ROT} = (ds)\left[\ln\left(\frac{CR+\Delta CR}{CR-\Delta CR}\right)\right]$

$\rho_{bROT} = D\rho_L + E\rho_S + F\Delta\rho_{ROT}$

ρ_L = LONG SPACING DENSITY

ρ_S = SHORT SPACING DENSITY

FIG.10D-1

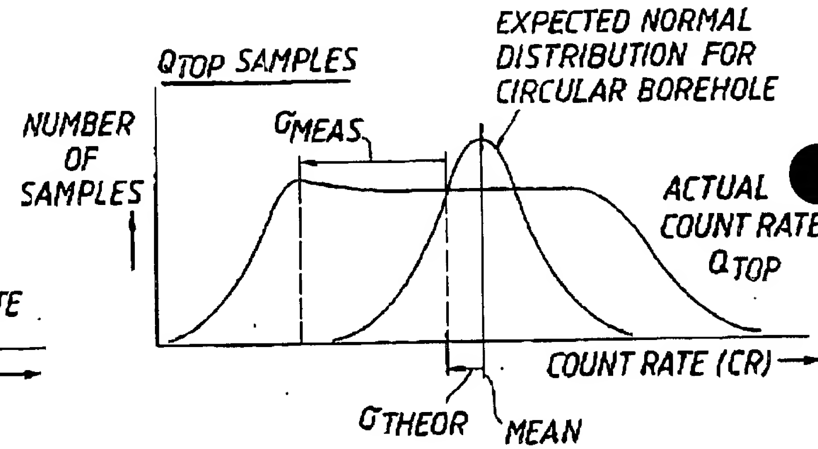

$\Delta CR_{TOP} = A\sqrt{\sigma^2_{MEAS_{TOP}} - \sigma^2_{THEOR_{TOP}}}$

$\Delta\rho_{ROT_{TOP}} = (ds)\left[\ln\left(\frac{CR_{TOP} + \Delta CR_{TOP}}{CR_{TOP} - \Delta CR_{TOP}}\right)\right]$

$\rho_{bROT_{TOP}} = D\rho_{L_{TOP}} + E\rho_{S_{TOP}} + F\Delta\rho_{ROT_{TOP}}$

$\rho_{L_{TOP}}$ = LONG SPACING DENSITY $_{TOP}$

$\rho_{S_{TOP}}$ = SHORT SPACING DENSITY $_{TOP}$

FIG.10D-2

FIG.11A

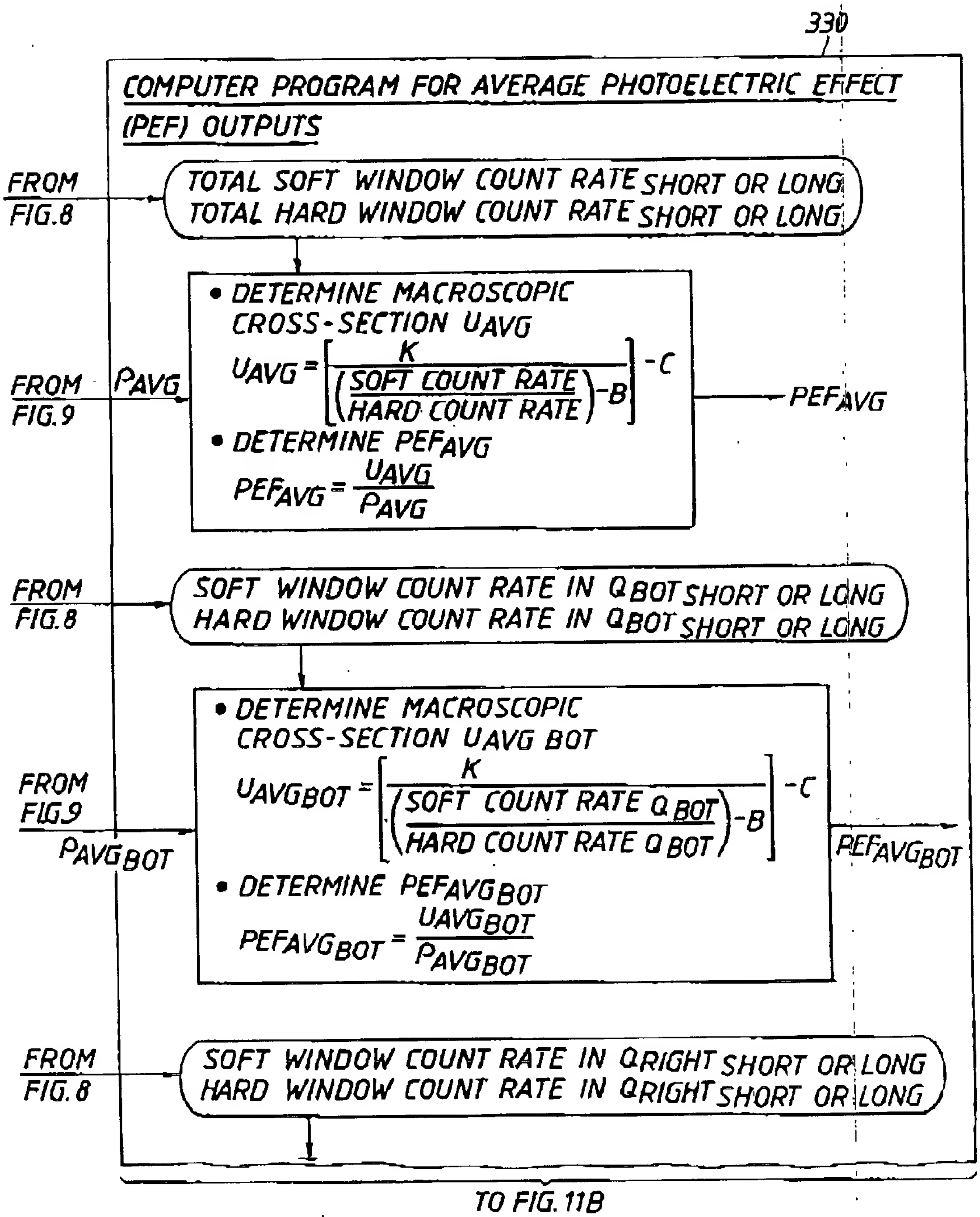
330
COMPUTER PROGRAM FOR AVERAGE PHOTOELECTRIC EFFECT (PEF) OUTPUTS
FROM FIG.8
TOTAL SOFT WINDOW COUNT RATE SHORT OR LONG
TOTAL HARD WINDOW COUNT RATE SHORT OR LONG
• DETERMINE MACROSCOPIC CROSS-SECTION UAVG
UAVG = [K / ((SOFT COUNT RATE / HARD COUNT RATE) - B)] - C
• DETERMINE PEFAVG
PEFAVG = UAVG / PAVG
FROM FIG.9
PAVG
PEFAVG
FROM FIG.8
SOFT WINDOW COUNT RATE IN QBOT SHORT OR LONG
HARD WINDOW COUNT RATE IN QBOT SHORT OR LONG
• DETERMINE MACROSCOPIC CROSS-SECTION UAVG BOT
UAVGBOT = [K / ((SOFT COUNT RATE Q BOT / HARD COUNT RATE Q BOT) - B)] - C
• DETERMINE PEFAVGBOT
PEFAVGBOT = UAVGBOT / PAVGBOT
FROM FIG.9
PAVGBOT
PEFAVGBOT
FROM FIG.8
SOFT WINDOW COUNT RATE IN QRIGHT SHORT OR LONG
HARD WINDOW COUNT RATE IN QRIGHT SHORT OR LONG
TO FIG.11B

FIG.11B

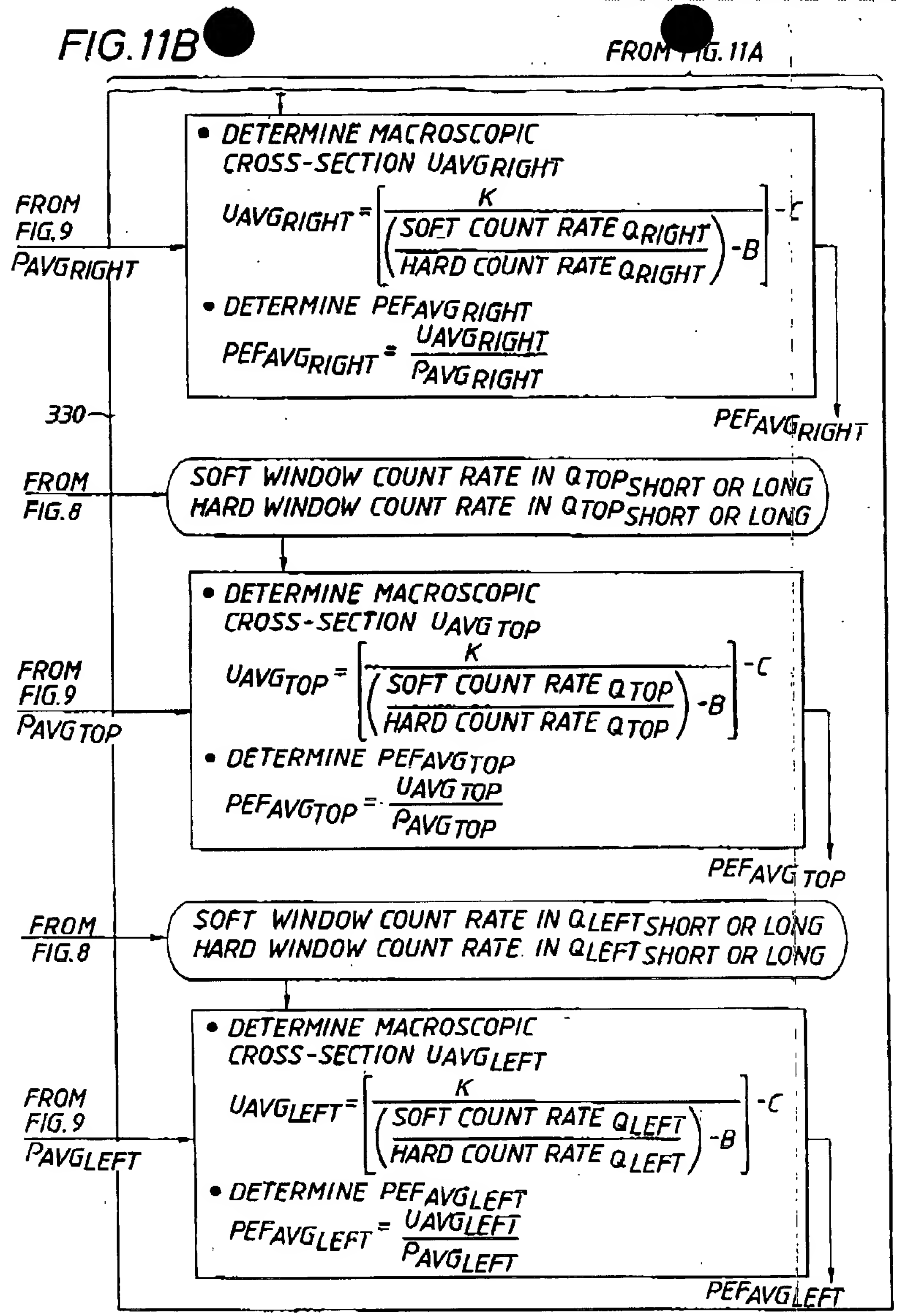
FROM FIG.11A
FROM FIG.9
PAVGRIGHT
• DETERMINE MACROSCOPIC CROSS-SECTION UAVGRIGHT
UAVGRIGHT = [K / ((SOFT COUNT RATE QRIGHT / HARD COUNT RATE QRIGHT) - B)] - C
• DETERMINE PEFAVGRIGHT
PEFAVGRIGHT = UAVGRIGHT / PAVGRIGHT
330
PEFAVGRIGHT
FROM FIG.8
SOFT WINDOW COUNT RATE IN QTOPSHORT OR LONG
HARD WINDOW COUNT RATE IN QTOPSHORT OR LONG
FROM FIG.9
PAVGTOP
• DETERMINE MACROSCOPIC CROSS-SECTION UAVGTOP
UAVGTOP = [K / ((SOFT COUNT RATE QTOP / HARD COUNT RATE QTOP) - B)] - C
• DETERMINE PEFAVGTOP
PEFAVGTOP = UAVGTOP / PAVGTOP
PEFAVGTOP
FROM FIG.8
SOFT WINDOW COUNT RATE IN QLEFTSHORT OR LONG
HARD WINDOW COUNT RATE IN QLEFTSHORT OR LONG
FROM FIG.9
PAVGLEFT
• DETERMINE MACROSCOPIC CROSS-SECTION UAVGLEFT
UAVGLEFT = [K / ((SOFT COUNT RATE QLEFT / HARD COUNT RATE QLEFT) - B)] - C
• DETERMINE PEFAVGLEFT
PEFAVGLEFT = UAVGLEFT / PAVGLEFT
PEFAVGLEFT

FIG. 12A

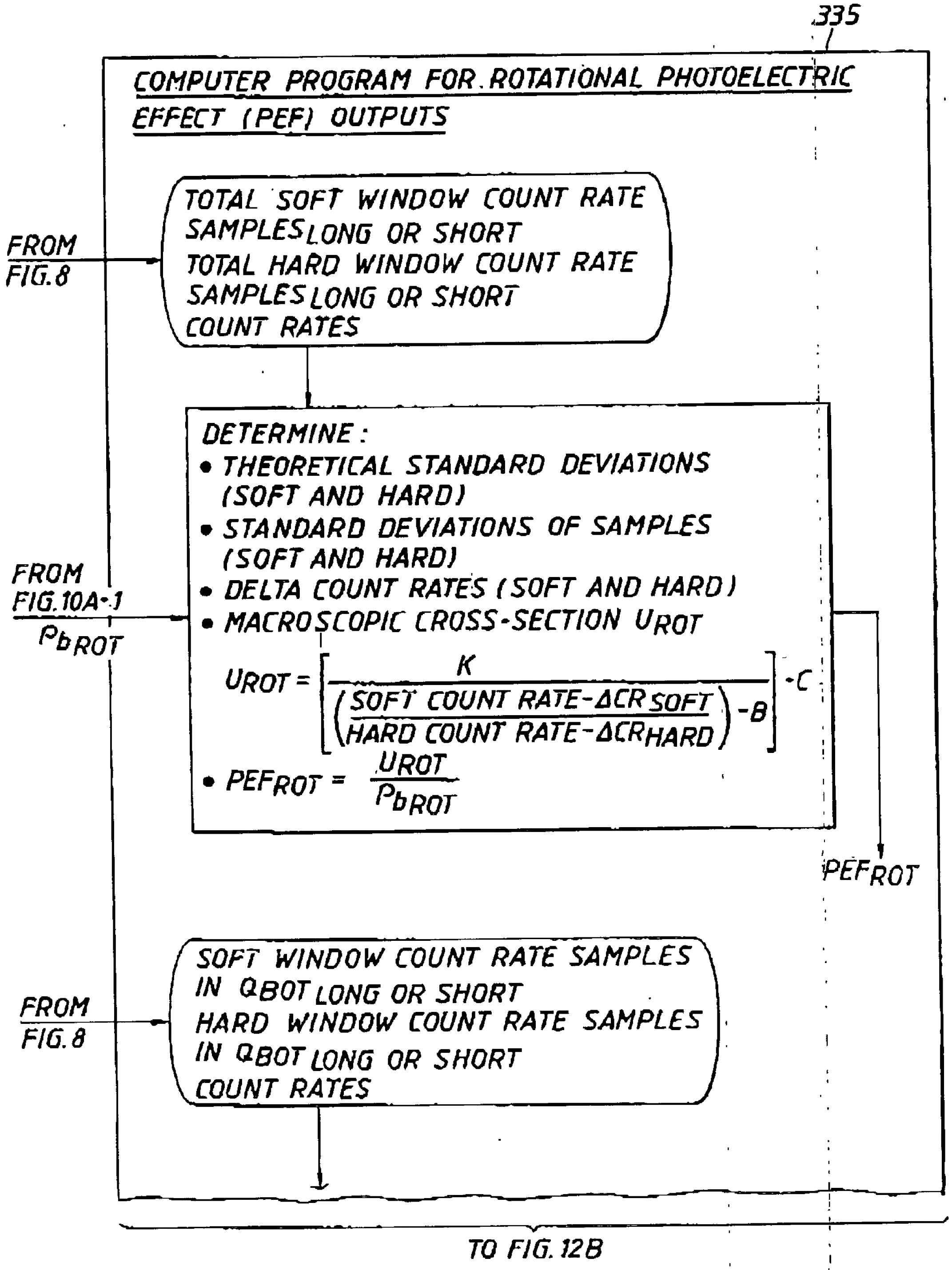
335
COMPUTER PROGRAM FOR ROTATIONAL PHOTOELECTRIC EFFECT (PEF) OUTPUTS
FROM FIG. 8
TOTAL SOFT WINDOW COUNT RATE SAMPLES LONG OR SHORT
TOTAL HARD WINDOW COUNT RATE SAMPLES LONG OR SHORT
COUNT RATES
FROM FIG. 10A-1
$P_{b\,ROT}$
DETERMINE:
• THEORETICAL STANDARD DEVIATIONS (SOFT AND HARD)
• STANDARD DEVIATIONS OF SAMPLES (SOFT AND HARD)
• DELTA COUNT RATES (SOFT AND HARD)
• MACROSCOPIC CROSS-SECTION U_{ROT}
$U_{ROT} = \left[\dfrac{K}{\left(\dfrac{\text{SOFT COUNT RATE} - \Delta CR_{SOFT}}{\text{HARD COUNT RATE} - \Delta CR_{HARD}} \right) - B} \right] \cdot C$
• $PEF_{ROT} = \dfrac{U_{ROT}}{P_{b\,ROT}}$
PEF_{ROT}
FROM FIG. 8
SOFT WINDOW COUNT RATE SAMPLES IN QBOT LONG OR SHORT
HARD WINDOW COUNT RATE SAMPLES IN QBOT LONG OR SHORT
COUNT RATES
TO FIG. 12B

FIG.12B

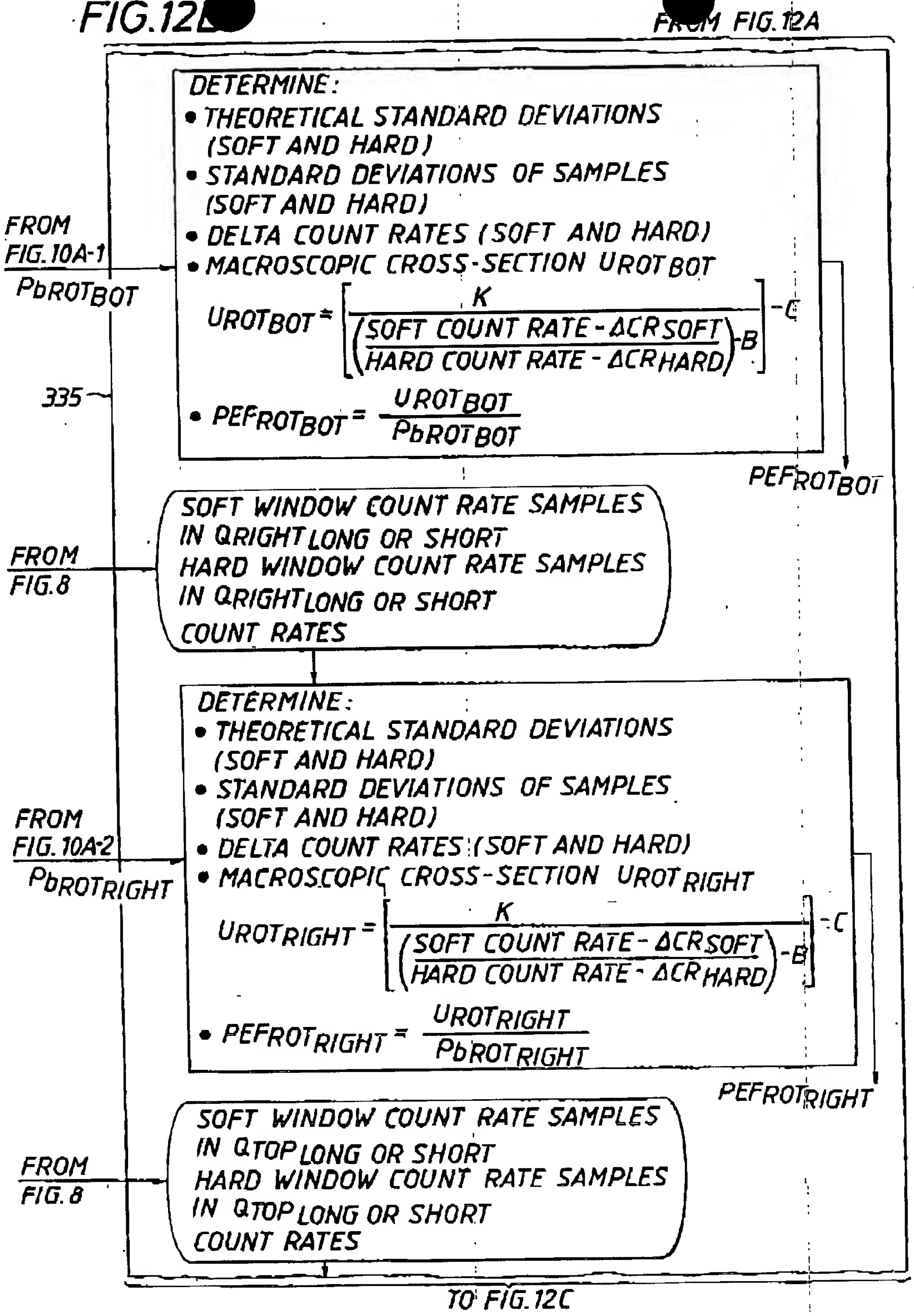
FROM FIG.12A
DETERMINE:
• THEORETICAL STANDARD DEVIATIONS (SOFT AND HARD)
• STANDARD DEVIATIONS OF SAMPLES (SOFT AND HARD)
• DELTA COUNT RATES (SOFT AND HARD)
• MACROSCOPIC CROSS-SECTION U_{ROTBOT}
$U_{ROTBOT} = \left[\frac{K}{\left(\frac{\text{SOFT COUNT RATE} - \Delta CR_{SOFT}}{\text{HARD COUNT RATE} - \Delta CR_{HARD}}\right) - B}\right] - C$
• $PEF_{ROTBOT} = \frac{U_{ROTBOT}}{Pb_{ROTBOT}}$
FROM FIG.10A-1
Pb_{ROTBOT}
335
PEF_{ROTBOT}
SOFT WINDOW COUNT RATE SAMPLES IN Q_{RIGHT} LONG OR SHORT
HARD WINDOW COUNT RATE SAMPLES IN Q_{RIGHT} LONG OR SHORT
COUNT RATES
FROM FIG.8
DETERMINE:
• THEORETICAL STANDARD DEVIATIONS (SOFT AND HARD)
• STANDARD DEVIATIONS OF SAMPLES (SOFT AND HARD)
• DELTA COUNT RATES (SOFT AND HARD)
• MACROSCOPIC CROSS-SECTION $U_{ROTRIGHT}$
$U_{ROTRIGHT} = \left[\frac{K}{\left(\frac{\text{SOFT COUNT RATE} - \Delta CR_{SOFT}}{\text{HARD COUNT RATE} - \Delta CR_{HARD}}\right) - B}\right] - C$
• $PEF_{ROTRIGHT} = \frac{U_{ROTRIGHT}}{Pb_{ROTRIGHT}}$
FROM FIG.10A-2
$Pb_{ROTRIGHT}$
$PEF_{ROTRIGHT}$
SOFT WINDOW COUNT RATE SAMPLES IN Q_{TOP} LONG OR SHORT
HARD WINDOW COUNT RATE SAMPLES IN Q_{TOP} LONG OR SHORT
COUNT RATES
FROM FIG.8
TO FIG.12C

FIG.1

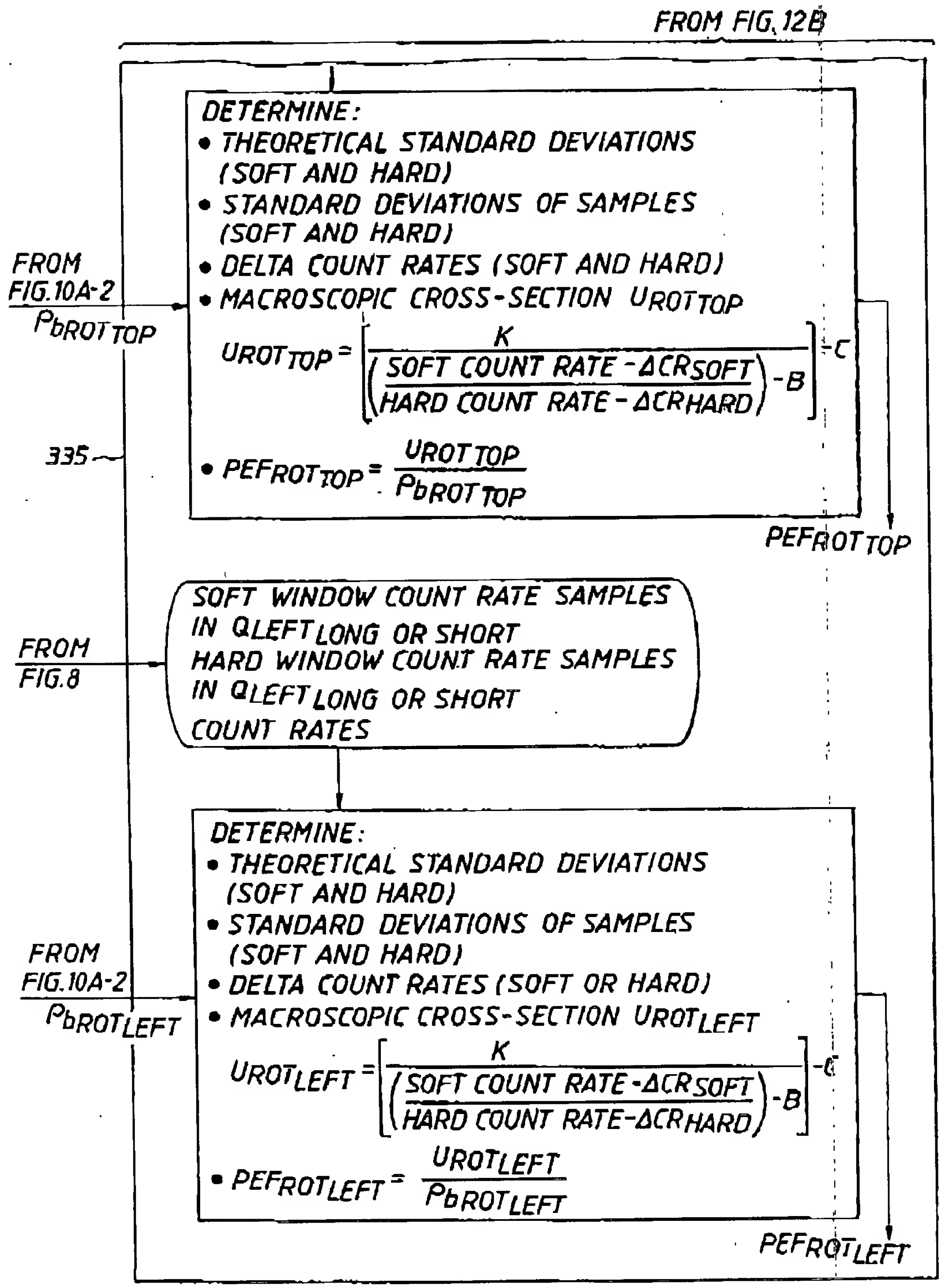
FROM FIG.12B
DETERMINE:
• THEORETICAL STANDARD DEVIATIONS (SOFT AND HARD)
• STANDARD DEVIATIONS OF SAMPLES (SOFT AND HARD)
• DELTA COUNT RATES (SOFT AND HARD)
• MACROSCOPIC CROSS-SECTION U_{ROTTOP}
$U_{ROTTOP} = \left[\frac{K}{\left(\frac{\text{SOFT COUNT RATE} - \Delta CR_{SOFT}}{\text{HARD COUNT RATE} - \Delta CR_{HARD}}\right) - B}\right] - C$
• $PEF_{ROTTOP} = \frac{U_{ROTTOP}}{P_{bROTTOP}}$
FROM FIG.10A-2
$P_{bROTTOP}$
335
PEF_{ROTTOP}
SOFT WINDOW COUNT RATE SAMPLES IN Q_{LEFT} LONG OR SHORT
HARD WINDOW COUNT RATE SAMPLES IN Q_{LEFT} LONG OR SHORT
COUNT RATES
FROM FIG.8
DETERMINE:
• THEORETICAL STANDARD DEVIATIONS (SOFT AND HARD)
• STANDARD DEVIATIONS OF SAMPLES (SOFT AND HARD)
• DELTA COUNT RATES (SOFT OR HARD)
• MACROSCOPIC CROSS-SECTION $U_{ROTLEFT}$
$U_{ROTLEFT} = \left[\frac{K}{\left(\frac{\text{SOFT COUNT RATE} - \Delta CR_{SOFT}}{\text{HARD COUNT RATE} - \Delta CR_{HARD}}\right) - B}\right] - C$
• $PEF_{ROTLEFT} = \frac{U_{ROTLEFT}}{P_{bROTLEFT}}$
FROM FIG.10A-2
$P_{bROTLEFT}$
$PEF_{ROTLEFT}$

FIG. 12D

335

COMPUTER PROGRAM FOR ROTATIONAL PHOTOELECTRIC EFFECT (PEF) OUTPUTS

FROM FIG. 8

TOTAL SOFT WINDOW COUNT RATE SAMPLES$_{LNG. OR SHT.}$
TOTAL HARD WINDOW COUNT RATE SAMPLES$_{LNG. OR SHT.}$
ACQUISITION TIME SAMPLES

- DETERMINE MACROSCOPIC CROSS-SECTION U's AS A FUNCTION OF ACQUISITION TIME

$$U_t = \left[\frac{K}{\left(\frac{\text{SOFT COUNT RATE}}{\text{HARD COUNT RATE}}\right) - B} \right] - C$$

- DETERMINE STANDARD DEVIATION FROM U_t's
- DETERMINE PEF_{ROT} FROM DISTRIBUTION OF U_t's

PEF_{ROT}

FROM FIG. 8

SOFT WINDOW COUNT RATE SAMPLES IN $Q_{BOT\,LNG. OR SHT.}$
HARD WINDOW COUNT RATE SAMPLES IN $Q_{BOT\,LNG. OR SHT.}$
ACQUISITION TIME SAMPLES

- DETERMINE MACROSCOPIC CROSS-SECTION U_{BOT}'s AS A FUNCTION OF ACQUISITION TIME

$$U_{t\,BOT} = \left[\frac{K}{\left(\frac{\text{SOFT COUNT RATE}}{\text{HARD COUNT RATE}}\right) - B} \right] - C$$

- DETERMINE STANDARD DEVIATION FROM $U_{t\,BOT}$'s
- DETERMINE $PEF_{ROT\,BOT}$ FROM DISTRIBUTION OF $U_{t\,BOT}$'s

$PEF_{ROT\,BOT}$

TO FIG. 12E

FIG.12E

FROM FIG.12D

FROM FIG.8

SOFT WINDOW COUNT RATE SAMPLES IN Q_{RIGHT} LNG. OR SHT.
HARD WINDOW COUNT RATE SAMPLES IN Q_{RIGHT} LNG. OR SHT.
ACQUISITION TIME SAMPLES

335

- DETERMINE MACROSCOPIC CROSS-SECTION U_{RIGHT}'s AS A FUNCTION OF ACQUISITION TIME

$$Ut_{RIGHT} = \left[\frac{K}{\left(\frac{\text{SOFT COUNT RATE}}{\text{HARD COUNT RATE}} \right) - B} \right] - C$$

- DETERMINE STANDARD DEVIATION FROM Ut_{RIGHT}'s
- DETERMINE $PEF_{ROTRIGHT}$ FROM DISTRIBUTION OF Ut_{RIGHT}'s

→ $PEF_{ROTRIGHT}$

FROM FIG.8

SOFT WINDOW COUNT RATE SAMPLES IN Q_{TOP} LNG. OR SHT.
HARD WINDOW COUNT RATE SAMPLES IN Q_{TOP} LNG. OR SHT.
ACQUISITION TIME SAMPLES

- DETERMINE MACROSCOPIC CROSS-SECTION U_{TOP}'s AS A FUNCTION OF ACQUISITION TIME

$$Ut_{TOP} = \left[\frac{K}{\left(\frac{\text{SOFT COUNT RATE}}{\text{HARD COUNT RATE}} \right) - B} \right] - C$$

- DETERMINE STANDARD DEVIATION FROM Ut_{TOP}'s
- DETERMINE $PEF_{ROT\,TOP}$ FROM DISTRIBUTION OF Ut_{TOP}'s

→ PEF_{ROTTOP}

TO FIG.12F

FIG. 12F

FROM FIG. 12E

FROM FIG. 8

SOFT WINDOW COUNT RATE SAMPLES IN Q_{LEFT} LNG. OR SHT.
HARD WINDOW COUNT RATE SAMPLES IN Q_{LEFT} LNG. OR SHT.
ACQUISITION TIME SAMPLES

335

- DETERMINE MACROSCOPIC CROSS-SECTION U_{LEFT}'s AS A FUNCTION OF ACQUISITION TIME

$$U_{tLEFT} = \left[\frac{K}{\left(\frac{\text{SOFT COUNT RATE}}{\text{HARD COUNT RATE}} \right) - B} \right] - C$$

- DETERMINE STANDARD DEVIATION FROM U_{tLEFT}'s
- DETERMINE $PEFROT_{LEFT}$ FROM DISTRIBUTION OF U_{tLEFT}'s

$PEFROT_{LEFT}$

FIG. 13

350

COMPUTER PROGRAM FOR ULTRASONIC STANDOFF OUTPUTS

FROM FIG. 4A-B

- RECORD STANDOFF AS A FUNCTION OF QUADRANT
- DEVELOP HISTOGRAM OF ALL STANDOFFS AND HISTOGRAM OF STANDOFFS PER QUADRANT
- DETERMINE $STANDOFF_{AVG}$, $STANDOFF_{MAX}$, $STANDOFF_{MIN}$ FOR EACH QUADRANT
- DETERMINE HOLE SHAPE:
  HORIZONTAL DIAMETER → H DIAMETER
  VERTICAL DIAMETER → V DIAMETER

FIG.14A

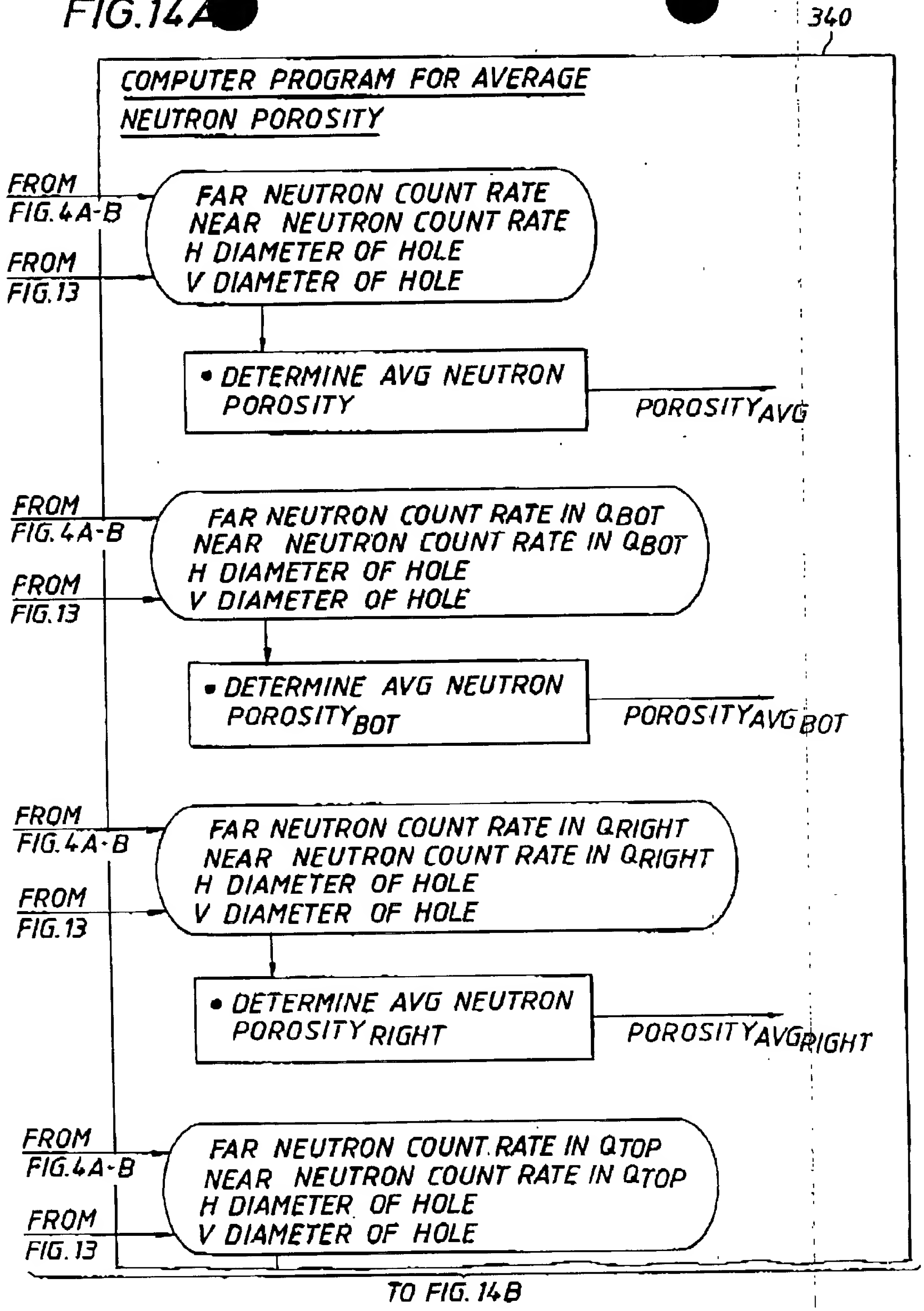
340
COMPUTER PROGRAM FOR AVERAGE NEUTRON POROSITY
FROM FIG.4A-B
FROM FIG.13
FAR NEUTRON COUNT RATE
NEAR NEUTRON COUNT RATE
H DIAMETER OF HOLE
V DIAMETER OF HOLE
• DETERMINE AVG NEUTRON POROSITY
POROSITY$_{AVG}$
FROM FIG.4A-B
FROM FIG.13
FAR NEUTRON COUNT RATE IN Q$_{BOT}$
NEAR NEUTRON COUNT RATE IN Q$_{BOT}$
H DIAMETER OF HOLE
V DIAMETER OF HOLE
• DETERMINE AVG NEUTRON POROSITY$_{BOT}$
POROSITY$_{AVG\ BOT}$
FROM FIG.4A-B
FROM FIG.13
FAR NEUTRON COUNT RATE IN Q$_{RIGHT}$
NEAR NEUTRON COUNT RATE IN Q$_{RIGHT}$
H DIAMETER OF HOLE
V DIAMETER OF HOLE
• DETERMINE AVG NEUTRON POROSITY$_{RIGHT}$
POROSITY$_{AVG\ RIGHT}$
FROM FIG.4A-B
FROM FIG.13
FAR NEUTRON COUNT RATE IN Q$_{TOP}$
NEAR NEUTRON COUNT RATE IN Q$_{TOP}$
H DIAMETER OF HOLE
V DIAMETER OF HOLE
TO FIG. 14B

FIG. 14B

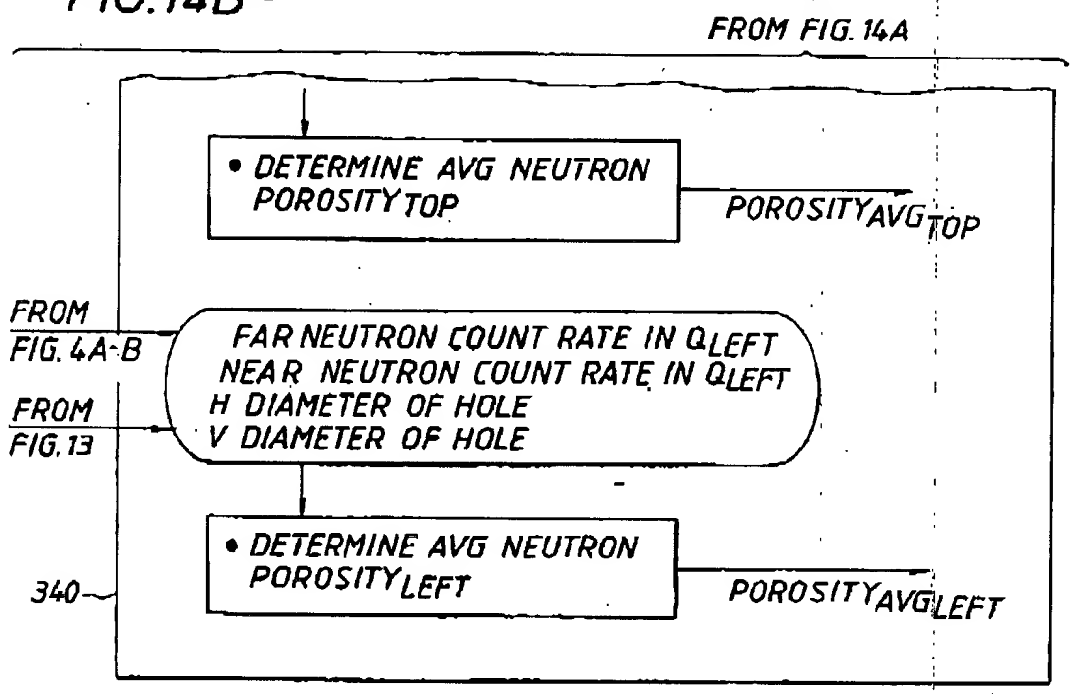

FIG. 15A

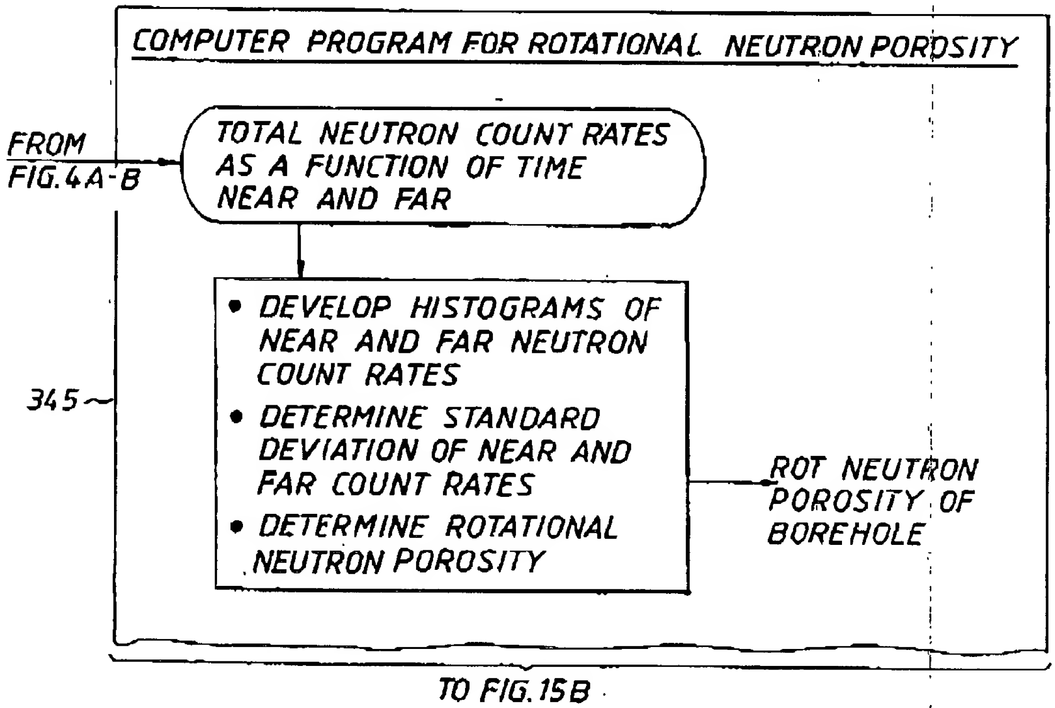

FIG.15B

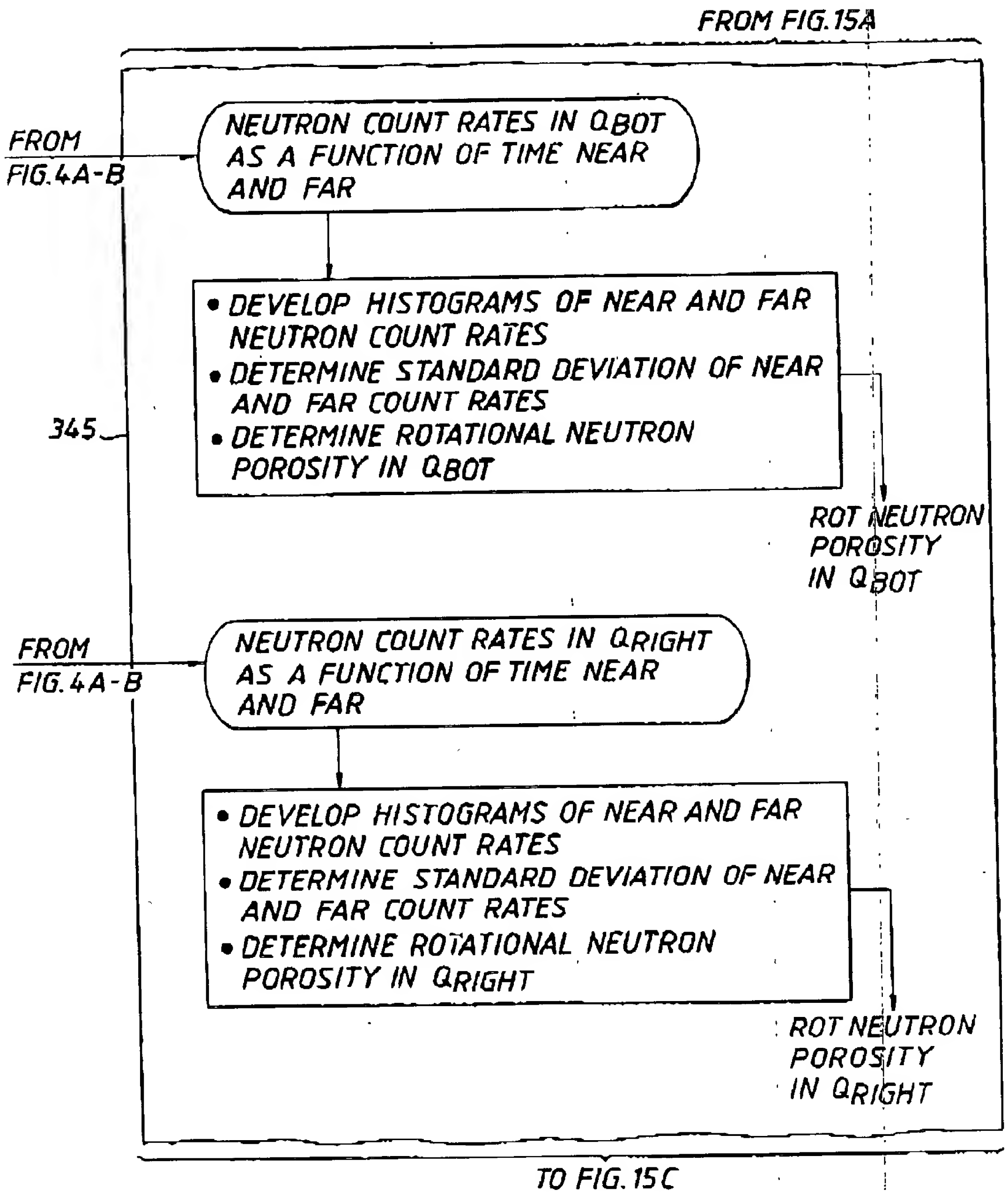
FROM FIG.15A
FROM FIG.4A-B
NEUTRON COUNT RATES IN QBOT AS A FUNCTION OF TIME NEAR AND FAR
• DEVELOP HISTOGRAMS OF NEAR AND FAR NEUTRON COUNT RATES
• DETERMINE STANDARD DEVIATION OF NEAR AND FAR COUNT RATES
• DETERMINE ROTATIONAL NEUTRON POROSITY IN QBOT
345
ROT NEUTRON POROSITY IN QBOT
FROM FIG.4A-B
NEUTRON COUNT RATES IN QRIGHT AS A FUNCTION OF TIME NEAR AND FAR
• DEVELOP HISTOGRAMS OF NEAR AND FAR NEUTRON COUNT RATES
• DETERMINE STANDARD DEVIATION OF NEAR AND FAR COUNT RATES
• DETERMINE ROTATIONAL NEUTRON POROSITY IN QRIGHT
ROT NEUTRON POROSITY IN QRIGHT
TO FIG.15C

FIG. 15C

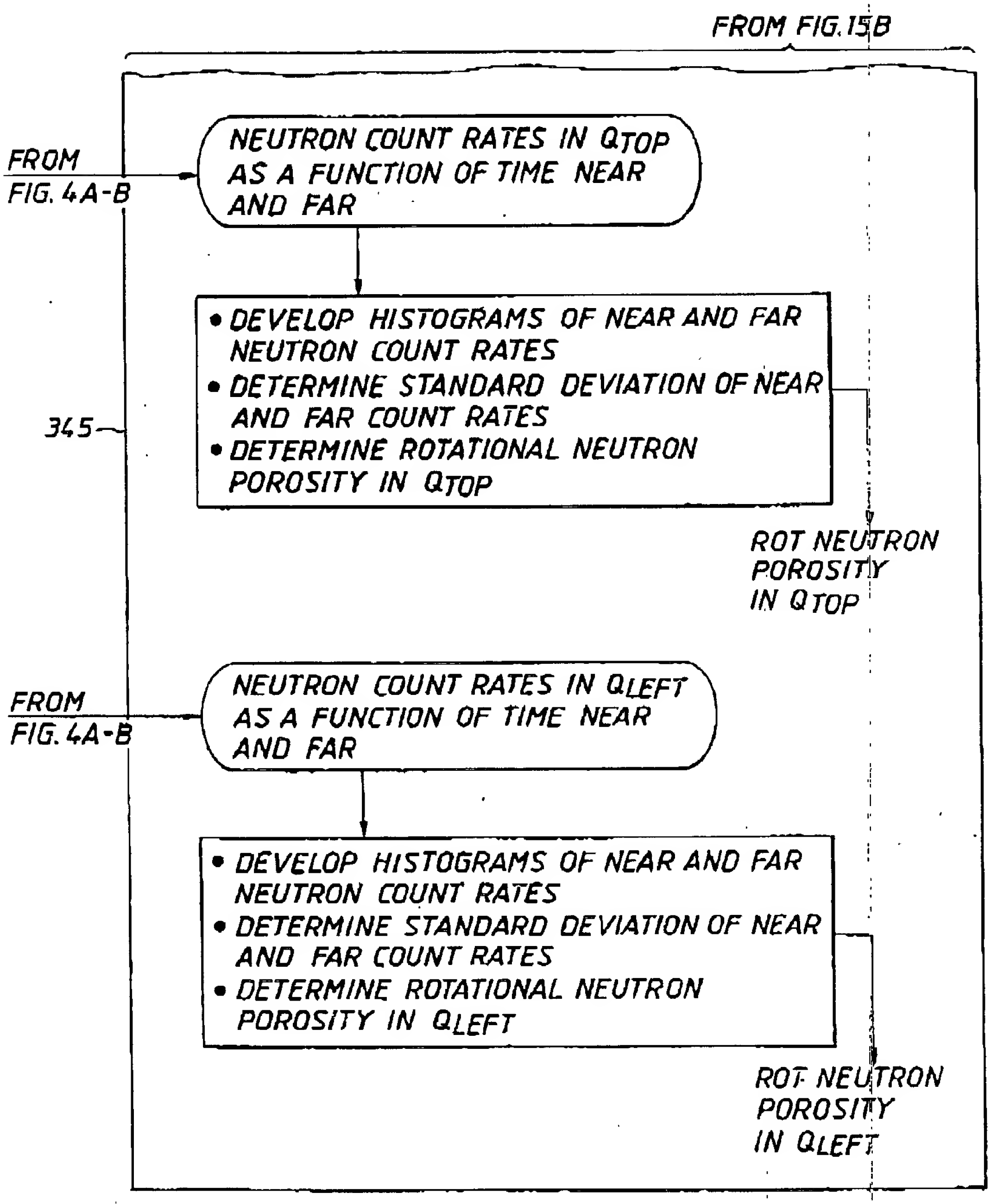
FROM FIG. 15B
FROM FIG. 4A-B
NEUTRON COUNT RATES IN QTOP AS A FUNCTION OF TIME NEAR AND FAR
• DEVELOP HISTOGRAMS OF NEAR AND FAR NEUTRON COUNT RATES
• DETERMINE STANDARD DEVIATION OF NEAR AND FAR COUNT RATES
• DETERMINE ROTATIONAL NEUTRON POROSITY IN QTOP
345
ROT NEUTRON POROSITY IN QTOP
FROM FIG. 4A-B
NEUTRON COUNT RATES IN QLEFT AS A FUNCTION OF TIME NEAR AND FAR
• DEVELOP HISTOGRAMS OF NEAR AND FAR NEUTRON COUNT RATES
• DETERMINE STANDARD DEVIATION OF NEAR AND FAR COUNT RATES
• DETERMINE ROTATIONAL NEUTRON POROSITY IN QLEFT
ROT NEUTRON POROSITY IN QLEFT

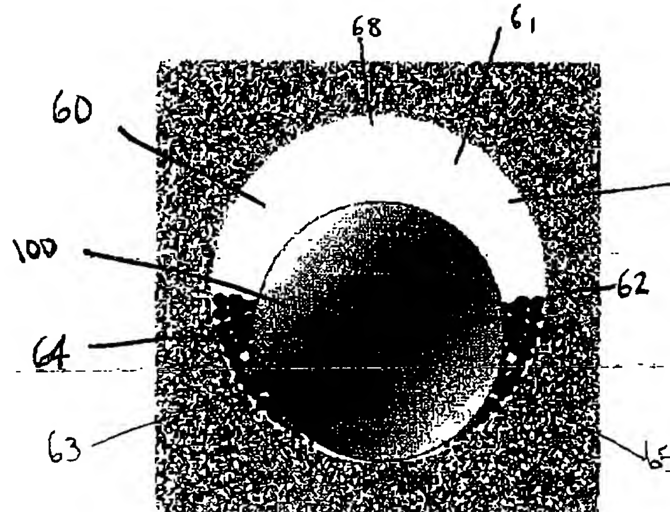

Figure 16A

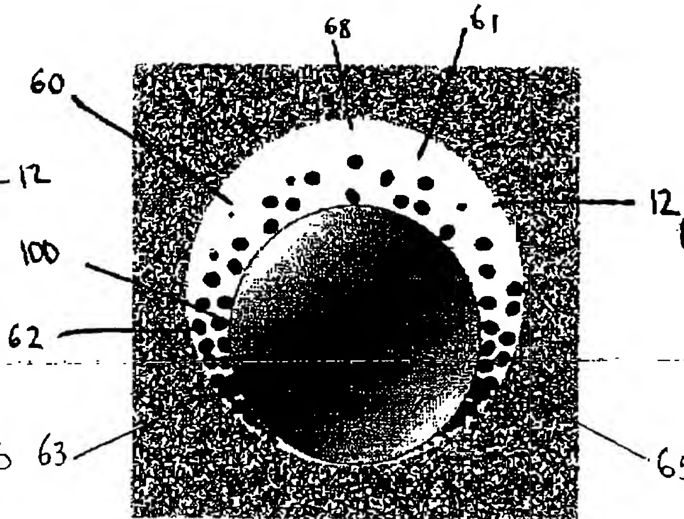

Figure 16B

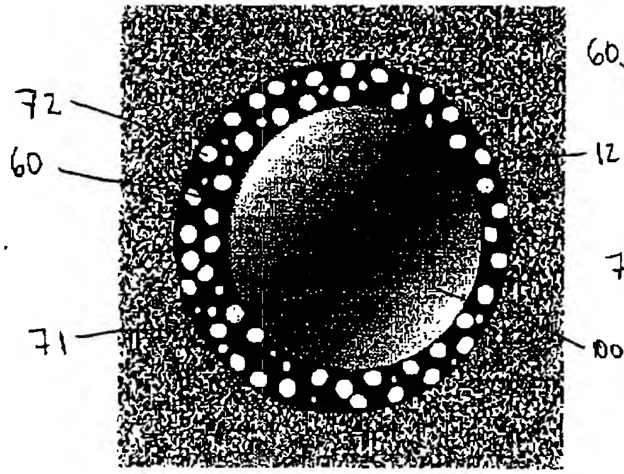

Figure 17A

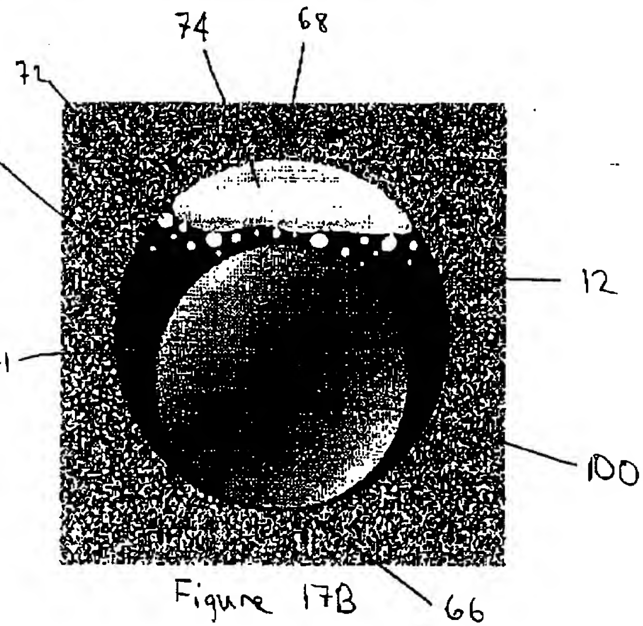

Figure 17B